Two-dimensional structural phase transitions in the stage-1 OsF_6-graphite intercalated compound

J. K. Kjems
Risø National Laboratory, P.O.B. 4000, Roskilde DK-4000, Denmark

Y. Yeshurun
Department of Physics, Bar-Ilan University, Ramat-Gan 52100, Israel

D. Vaknin and D. Davidov
Racah Institute of Physics, Hebrew University, Jerusalem, Israel

H. Selig
Department of Chemistry, Hebrew University, Jerusalem, Israel
(Received 26 August 1986; revised manuscript received 9 June 1987)

Neutron scattering has been used to study the temperature dependence of the in-plane structure of the stage-1 graphite intercalation compound C_9OsF_6. The low-temperature structure has a two-dimensional character and can be described as a nearly hexagonal domain-wall lattice in which sharp domain walls separate regions of $(2\times2)R0°$ structure on a 60-Å scale. The domain-wall lattice is imperfect with a correlation length that only extends over a few such regions. The in-plane intercalant structure is disordered above 280 K and resistivity measurements show a clear hysteresis in the transition region above 250 K, indicating a first-order transition. The structural data are consistent with coexistence of a solidlike and fluidlike phase in the transition region, as expected for constant volume melting. The results suggest that this class of intercalation compounds is a good realization of a four-state Potts model with effective dimensionalities less than 3.

I. INTRODUCTION

Graphite intercalation compounds (GIC's) belong to the family of intergrowth compounds[1] consisting of two (or more) sublattices that can show radically different behavior with changing temperature. One sublattice, here the carbon, may remain fixed and rigid while the other undergoes a variety of transitions such as sublattice melting, order-disorder, and superlattice formation. Systems with differing natural periodicities are particularly interesting and may display a rich variety of commensurate-incommensurate transitions.[2–4] The intergrowth compounds often have effective dimensionalities lower than 3, and their properties can often be understood in terms of models of great theoretical interest since the reduced dimensionality in general makes the models more tractable.

GIC's can be synthesized with a varying number of graphite basal plane layers between the intercalant layers, denoted by the staging index, n. The high-n compounds have weaker coupling between the intercalant layers and can thus be expected to show near two-dimensional (2D) behavior, as indeed has been found, for example, for $C_{24}Cs$.[5] However, all stage-1 alkaline metal GIC's show 3D ordering and their transitions have to be analyzed accordingly.[6] This does not necessarily make them less interesting, as is evidenced by the study of C_6Li (Ref. 7) which documented the analogy to the lattice gas version of the 3D three-state Potts model for this system.

Here we present neutron diffraction and resistivity data for stage-1 C_9OsF_6 which belongs to a new class of GIC's with metal-hexafluoride intercalants.[8] So far most of the interest in these compounds has concerned the electronic and magnetic properties[9] which can be varied as a function of the intercalant metal (M=Os, Ir, Tc, Pt, Re, and Mo).[10] We chose to study the OsF_6 system in order to determine both the chemical structure and a possible ordered magnetic state at low temperatures.[8] No evidence for magnetic order was found, and this paper focuses on the structural study. We have found a modulated incommensurate (possibly high-order commensurate), low-temperature structure of the intercalant layers which transforms to a simpler incommensurate form at about 240 K before it becomes disordered above $T_M \simeq 270$ K. Pronounced hysteresis in the resistivity measurements reveals the first-order character of the transition at T_M. Our most important finding is the 2D character of the low-temperature structure with a strong preference for particular intercalant sites which suggests that this and other of the MF_6-GIC's may be good realizations of the lattice-gas version of the 2D four-state Potts model whose properties have been extensively studied theoretically[11] but for which no good experimental examples have been found so far. The different choices of MF_6 molecules in this series give somewhat different stoichiometries which correlate with the electron transfer. Hence there are good possibilities for systematic studies as a function of the intercalant density.

The remainder of the paper is organized as follows:

first we report the experimental details (Sec. II) and present our results (Sec. III), then the analysis of the low-temperature structure is presented (Sec. IV), and finally we discuss the phase transitions (Sec. V), and state our conclusions (Sec. VI).

II. EXPERIMENTAL PROCEDURE

A. Sample preparation

Highly oriented pyrolytic graphite (HOPG) in the form of a block ($5\times12\times2$ mm^3) was exposed to OsF_6 at room temperature (RT). The staging index ($n=1$) was determined by the diffraction from ($00l$) planes using Cu $K\alpha$ x-ray radiation. The intercalant species are almost completely in the form of OsF_6 units; i.e., there is a charge transfer of one electron per OsF_6 formula.[8–10] The samples were also characterized by the weight uptake.

B. Neutron diffraction

The neutron-diffraction experiment was carried out using a triple-axis spectrometer situated at a cold source beam at the Risø DR-3 reactor. For the initial scans a wavelength of 2.38 Å was used at which pyrolytic graphite filters are very efficient in removing any higher-order contamination. High-resolution scans were performed using a wavelength of 4.30 Å. A combination of a 10-cm cooled Be filter before the graphite (002) monochromator and a 5-cm graphite Be filter, placed before the sample, was used to remove higher orders in this case. The typical collimation was 60′ but occasionally 30′ was used before the monochromator and after the sample. The best resolution achieved was 0.0095 Å^{-1} full width at half maximum (FWHM) at $Q=1.470$ Å^{-1}, as determined from the $\lambda/2$ $(100)_G$ reflection. This Q value corresponds to a basal-plane lattice parameter $a_C=2.468\pm0.005$ Å, which is slightly larger than the literature values. The sample was mounted in a standard, sealed aluminum container, filled with He gas in a dry box. The c axis was in the horizontal scattering plane, and cooling was achieved by means of a closed-cycle Displex cryostat.

C. Resistivity measurements

The electrical resistivity along the c axis, ρ_c, was measured by the standard four-probe dc technique. Electrical contacts were made in the form of two nickel disks for the current injection and two platinum probes for measuring the voltage. Low temperature was attained by using an Air-Product closed-cycle refrigerator, and typical heating-cooling rates were 0.3 K/min.

III. RESULTS

A. Neutron diffraction

The neutron-diffraction scans along ($00l$) confirmed the stage-1 character of C_9OsF_6 as well as the known $c=8.10$ Å distance. The peaks associated with the carbon lattice were sharp in the longitudinal direction and the rocking curves have a mosaic width of 1.7° (FWHM). The intensities of the carbon (hkl) reflections confirmed the A-A stacking of the carbon layers. The structure of the intercalant layers was revealed by scans in the basal plane, $l=0$, which give powder-averaged intensities due to the pyrolytic nature of the HOPG. The low-temperature scans show a complex structure, with the most prominent peaks from the intercalants in the Q range 1–2 Å^{-1}. Examples of scans in this region obtained with intermediate resolution ($\lambda=2.36$ Å) for different temperatures are shown in Fig. 1. At low temperature, the scans show considerable structure around $q=1.4$ Å^{-1}, most of which disappears and develops into a broad peak above 300 K. Scans were also made in the range 2–5 Å^{-1} at $T=4.2$ K. Here, in contrast to the rich spectra of the lower Q range, the scans show surprisingly little scattering in the range 2–3.5 Å^{-1} and a series of weak peaks and features (at about 50% of the background intensity level) between 3.5 and 5 Å^{-1}. Apart from the expected reflections from the carbon lattice and the Al container, only a weak peak at 4.25 Å^{-1} was clearly resolved.

Most of the experiments were carried out at high resolution ($\lambda=4.48$ Å), and the scans were concentrated in the range 1–2 Å^{-1}, which appeared to give the most useful information. Examples of such scans are shown in Fig. 2, where one clearly resolves six stronger peaks and several weaker features at low temperature ($T=222$ K). The instrumental resolution is illustrated by the scan through the $(100)_C$ peak with the filters removed. The position of this peak corresponds to the $(10)_I$ reflection for a $(2\times2)R0°$ commensurate intercalant lattice, as will be discussed later in connection with Fig. 6. Scans were also performed along q_z at the q_x positions of

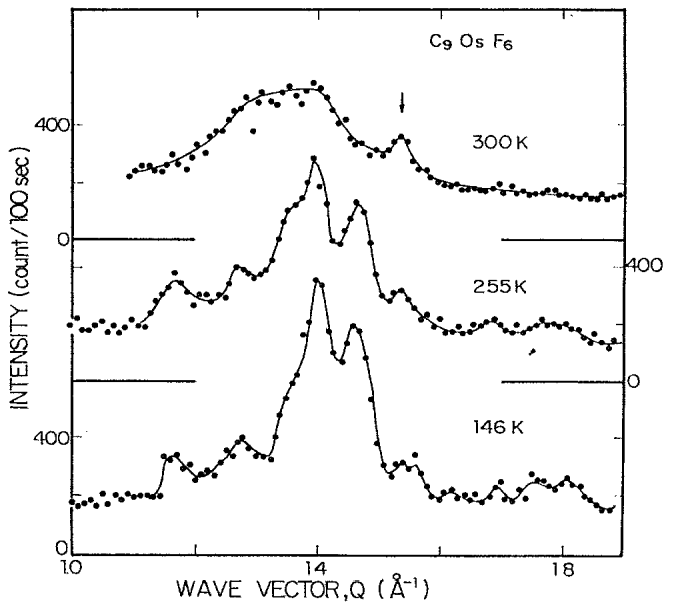

FIG. 1. Neutron-diffraction scans in the basal plane of HOPG stage-1 C_9OsF_6 at three different temperatures indicated. The neutron wavelength was 2.36 Å corresponding to an intermediate resolution.

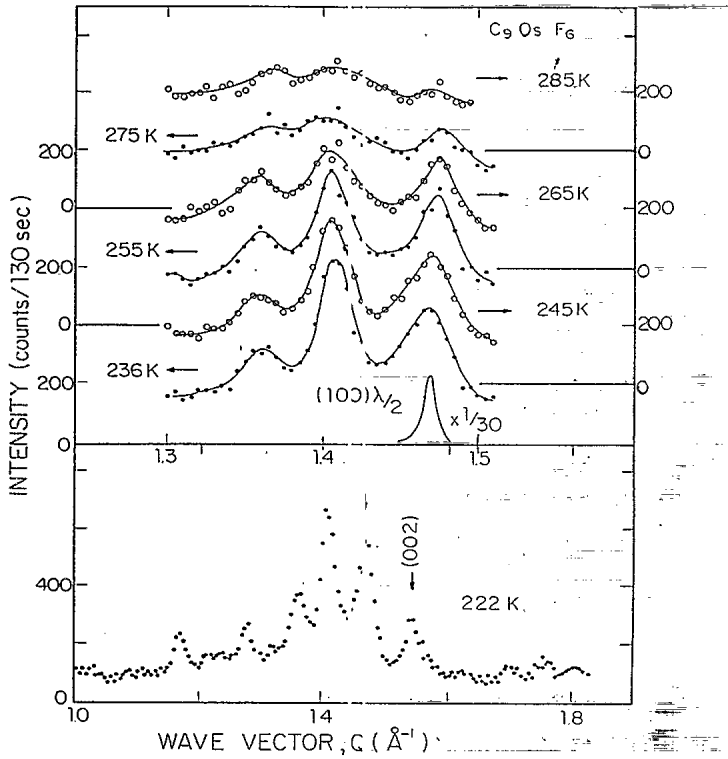

FIG. 2. High-resolution neutron-diffraction scans in the basal plane of HOPG stage-1 C_9OsF_6. The upper panels show the most intense peaks on an expanded scale at increasing temperature through the order-disorder melting transition of the intercalant layers. The arrow on the lower panel indicates a small (002) contribution caused by severely misoriented grains. In the upper panel the $\lambda/2$ scan of the $(100)_C$ peak is also shown, as an illustration of the instrumental resolution and of the commensurate position of the $(2\times2)R0°$ structure indicated by an arrow on the lower panel.

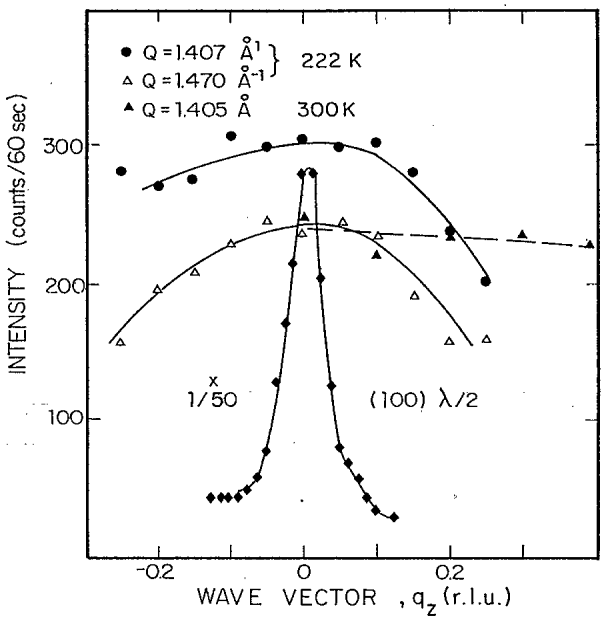

FIG. 3. Scans in the direction perpendicular to the basal plane at the positions of the most prominent basal-plane intercalant peaks in the low-temperature phase and of the $\lambda/2$ $(100)_G$ reflection from the carbon lattice. The weak q_C dependence of the intercalant peaks is indicative of a 2D structure as discussed in the text. Also shown are similar scans in the high-temperature disordered phase. The reduced units (r.l.u.) refer to the c axis unit, $\tau(001)=0.778$ Å^{-1}.

the most prominent peaks, and the results are plotted in Fig. 3. This clearly shows that the intensity is distributed in cylindrical sheets with their axes parallel to the c axis, a clear signature of a lattice of 2D nature. Similar scans taken at $T=300$ K are completely flat, whereas a weak modulation is observed at low temperatures, some of which could stem from resolution effects due to change in the intersection of the diffraction sheets and the resolution volume.

Figure 2 also shows examples of the temperature evolution of the most intense triplet (shown on expanded scale). It is seen that the peaks broaden, shift slightly, and gradually weaken in the temperature range 240–300 K. These trends have been quantified by Lorentzian fits to the peak at 1.47 Å^{-1}, and Fig. 4 summarizes the results for the peak intensity, width, and position. We note that all the peak widths exceeded the instrumental resolution (0.005 Å, HWHM) indicating an in-plane coherence length of the order of 60 Å at low temperatures.

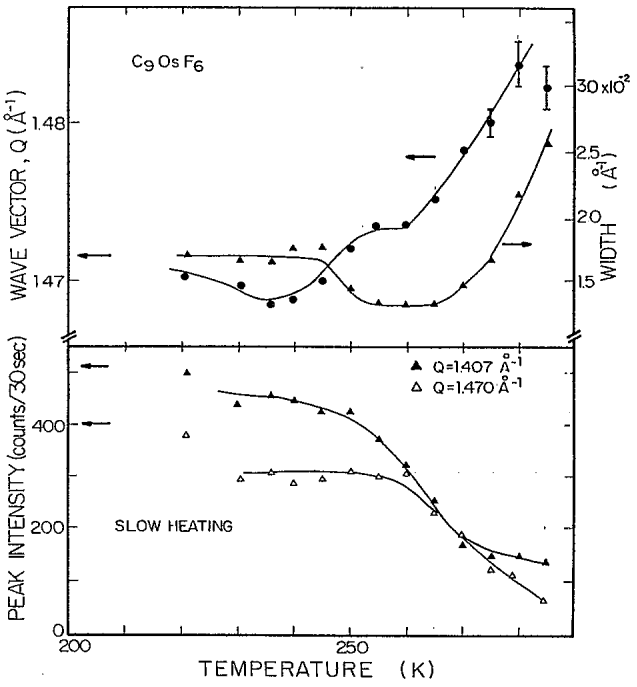

FIG. 4. Results of Lorentzian line profile fits to the peak near 1.47 Å in the basal plane versus temperature. The upper panel shows the position Q and width Γ. The lower panel also shows the peak intensity for the 1.407 Å^{-1} peak. The arrows indicate the low-temperature ($T=4.2$ K) values.

B. Resistivity

The c axis resistivity ρ_c shows an overall metalliclike behavior with a positive temperature coefficient (Fig. 5). $\rho_c(T)$ shows strong hysteresis which depends on the rate of cooling. The hysteresis loops were checked from RT to 50 K and showed the largest loop down to 220 K.

IV. STRUCTURAL ANALYSIS

A. Low-temperature phase

The previous diffraction studies of OsF_6 GIC used x rays at medium resolution,[8] and the results suggested that the in-plane structure was the well-known $(2\times2)R0°$, which is common for the alkali-metal GIC.[1] This structure would give a single peak at the commensurate $Q=1.468$ Å^{-1} position in the scans shown in Figs. 1 and 2. Clearly the structure is more complex. A simple incommensurate hexagonal intercalant lattice would also only yield a single peak in this Q range, so instead we propose a *modulated structure* which is the result of the interaction of an incommensurate intercalant lattice with $a_I=5.167$ Å $[\tau_I(10)=1.407$ Å$^{-1}]$ and the carbon basal-plane lattice with $a_C=2.468$ Å. In acceptor GIC's one usually finds a slight reduction of the carbon-carbon distance relative to the pure graphite. Here we find a value that is insignificantly larger than the literature values. However, we did not pursue this effect as a possible measure of the intercalant-graphite interaction. The lattice parameter mismatch for the intercalant lattice relative to the $(2\times2)R0°$ structure is 4.5%. In the simplest model this interaction results in a superstructure, often referred to as a soliton or domain-wall lattice which can be generated by the construction shown in Fig. 6(a). The basis of the superlattice is $\tau_s=\tau_C-2\tau_I$, and hence it depends on both the mismatch and on the relative orientation of the two primary lattices. The superlattice reflection decorates the primary lattice reflections with patterns of satellites

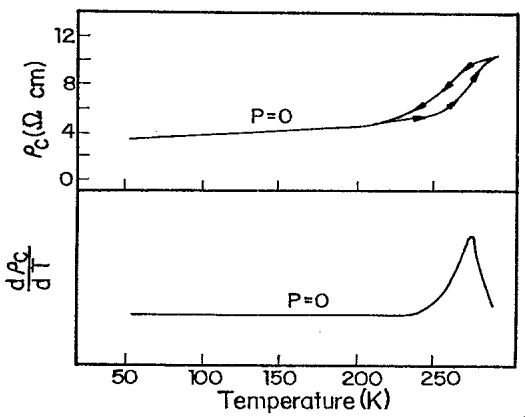

FIG. 5. Resistivity along the c axis vs temperature for stage-1 C_9OsF_6 at ambient pressure and its temperature derivatives. The changes above 250 K coincide with the order-disorder transition and the hysteresis indicate its first order nature.

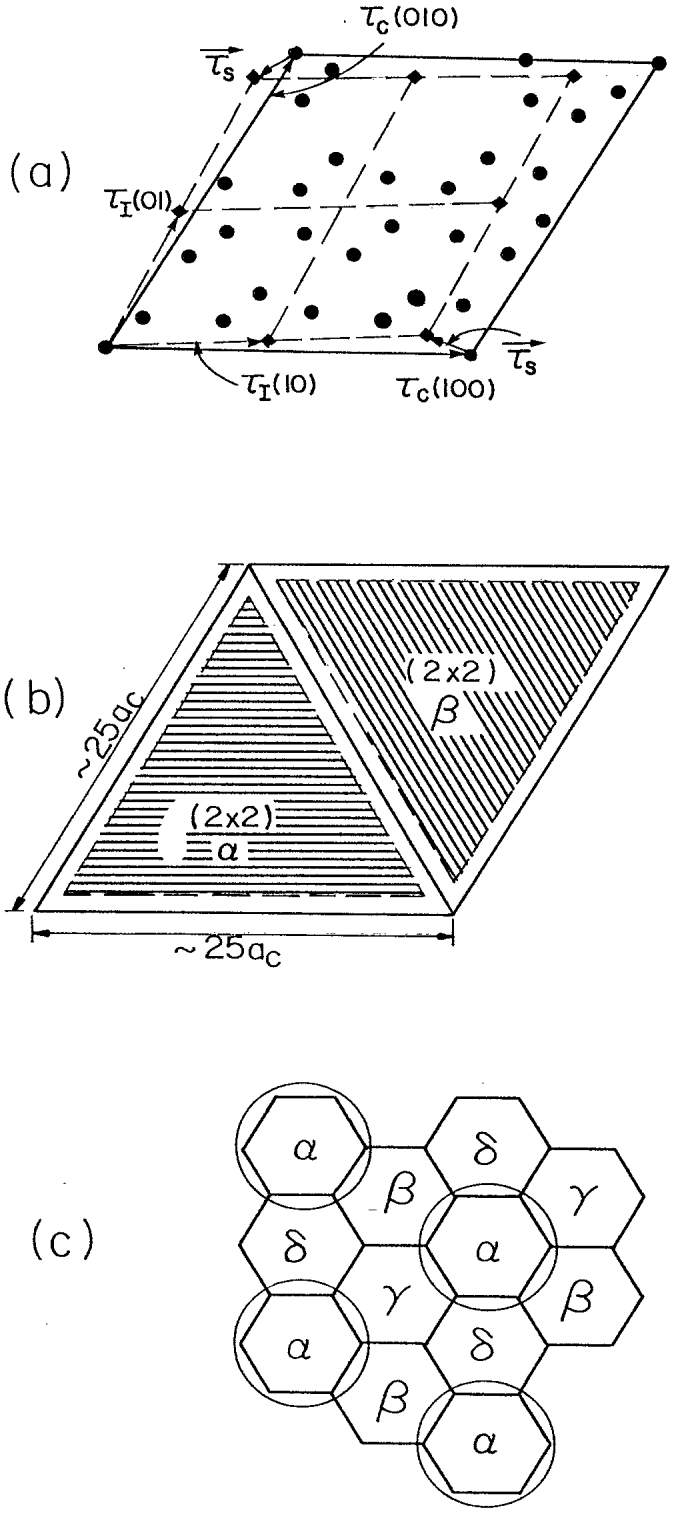

FIG. 6. (a) Construction of the possible superlattice reflections that result from the interaction of two incommensurate hexagonal lattices. τ_C describes the carbon lattice, τ_I the intercalant lattice, and τ_s the superlattice. (b) Schematic model of the domain-wall lattice with large triangular regions of commensurate (2×2) structure. This model explains qualitatively the observed neutron-diffraction profiles in the low-temperature phase. (c) Illustration of the $(2\times2)R0°$ structure with indication of the four sublattices and of the most probable OsF_6 sites.

whose structure factors will depend on the amounts of distortions that are induced by the mutual interactions. The calculated, powder-averaged, peak positions near $\tau_I(10)=1.407$ Å^{-1} are shown in Table I for the most prominent peaks. Already the simplest model 1, in which $\tau_I(10)$ is parallel to $\tau_C(100)$, shows a reasonable agreement with the observations. However, there are slight systematic differences and several modifications of the model were explored in order to explain these. Model 2 corresponds to a small relative rotation of the primary lattices (0.18°) which induces a much larger rotation (4.4°) of the superlattice. Model 3 corresponds to a small strain (shear) of the intercalant lattice which changes the symmetry from hexagonal to orthorhombic and changes the angle α from 60° to 59.8°. All three models preserve the relation $\tau_s=\tau_C-2\tau_I$, and they reproduce the observed positions reasonably well, so based on these alone it is difficult to make a distinct choice. A slight asymmetry in the shapes of the 1.36 and 1.47 Å^{-1} peaks could indicate a strained rather than a rotated superlattice which would be expected to result in symmetric splitting of these peaks. From the value of $|\tau_s|\simeq 0.12$ Å^{-1} we conclude that the nearly hexagonal domain-wall lattice has a unit cell of $a_s=60.5$ Å corresponding to approximately 25 carbon cell units, $a_C=2.68$ Å. The c axis scans shown in Fig. 3 indicate that there is little or no correlation between the domain-wall lattices in adjacent intercalant planes, implying a truly 2D nature of the ordering.

The observed intensity distributions have some overall features which can be explained in general terms. First, the absence of satellite intensities near the $\tau_I(11)$, $\tau_C(100)$, and $\tau_I(20)$ and the weak peak at $\tau_I(30)=4.25$ Å^{-1} is consistent with the variations expected on the basis of the OsF_6 molecular form factor given by

$$f(\tau)=\sum_i b_i e^{i\tau\cdot\rho_i},$$

where b_i is the scattering length and ρ_i denotes the position of the individual atoms in the molecule. Calculations assuming the threefold molecular axis parallel to the c axis showed, furthermore, that the intensities near $\tau_I(10)$ are determined solely by the molecular center of mass positions, i.e., that orientational effects can be neglected. Hence we can treat the molecules as isotropic units. Secondly, we note that the satellite intensities are comparable to the fundamental $\tau_I(10)$ reflection and that there are visible satellites up to orders greater than 3. This suggests that the domain walls are quite sharp and that they separate regions of nearly constant intermolecular spacings. This leads us to a model of the kind illustrated in Fig. 6(b) in which the domain-wall lattice unit cell contains triangular regions of registered $(2\times2)R0°$ structure with approximately 11 OsF_6 molecules along the edge. This would give a chemical composition of $C_{9.5}OsF_6$, consistent with the weight uptake during synthesis. The triangular regions are shifted consecutively from one sublattice to the next in the (2×2) [Fig. 6(c)] structure. The total structure factors calculated for different variants of this model, i.e., different combinations of α, β, γ, and δ sublattices show qualitative agreement with the observed intensities. In particular, they give the satellite and the fundamental peak intensities in the right proportions. The models are too crude to warrant refinement, but we believe they give a good qualitative picture of the domain-wall structure. The models also naturally explain small possible strains and rotations corresponding to the difference between various, nearly identical, forms of higher-order registry like (25,0) or (24,1) in notation that refers to the number of graphite hexagons between registry. The observed linewidths indicate that the domain-wall lattice loses its coherence after a few units, implying a near-random choice between the different higher-order commensurabilities. An important conclusion from this picture is that a large fraction, possibly all of the OsF_6 molecules, are located at high-symmetry sites of which the centers of the carbon rings are the most probable according to earlier suggestions.[8]

TABLE I. Observed and calculated peak positions for the most prominent peaks in the region near $Q=1.5$ Å^{-1}. The models are explained in the text. Models 2 and 3 correspond to distorted domain-wall lattices which lead to splitting of some of the peaks.

Observed peak positions (Å^{-1})	Calculated positions Model 1 (Å^{-1})	Model 2 (Å^{-1})	Model 3 (Å^{-1})
1.169	1.169	1.170	1.170
1.277	1.289	1.284	1.281
1.360	1.352	1.369 1.337	1.340 1.353
1.407	1.4085	1.4085	1.405
1.470	1.472	1.457 1.487	1.463 1.478

B. Temperature evolution

Above 300 K the intercalant lattice is disordered, although the data in Fig. 1 show some structure arising from short-range order effects reminiscent of the domain-wall lattice. The transition from the low-temperature phase upon heating appears to occur in two steps. The first is seen around 250 K, where the position of the peak at $Q=1.47$ Å^{-1} shifts slightly concomitantly with a small but significant decrease in the linewidth. The diffraction pattern at 260 K can be explained by a simple hexagonal, unstrained domain-wall lattice [like model 1]. The second step is a gradual melting in the temperature range 260–280 K. During this process the correlation length shrinks and the peak positions shift steadily towards higher q values. The diffraction data could be consistent with a coexistence of a solidlike and a fluidlike phase, but no attempts were made to quantify this by a line-shape analysis for which one would have to invoke three narrow and one broad peak.

V. DISCUSSION

The symmetry of the low-temperature structure corresponds to the distortion pattern that follows from the

simplest linear response to the mutual interaction of the two primary lattices with differing periodicity and/or orientations. In the continuum limit, this corresponds to the famed Frenkel–Kontorowa–Frank–van der Merwe (FKFM) model[12] which predicts smooth, regularly space solitonlike domain walls. However, the discreteness of the lattice is known to cause substantial deviation from the simple FKFM model behavior and can lead to a complete, or incomplete so-called devil's staircase of higher-order commensurate states as the mismatch between the two lattices is varied.[2] It has also been suggested that the system may be intrinsically unable to choose between the possible states and display a chaotic behavior. In the present case the density in the intercalant layers is constant, and only a limited range of mismatch is explored by the temperature variation before the system locks into the low-temperature, partly disordered structure. The disorder could stem from a random pinning of the domain-wall crossings at sites corresponding to different higher-order commensurate states and may hence be classified as chaotic. At temperatures near 260 K the domain-wall lattice appears to be less strained, although the correlation length as measured by the linewidth is still finite and it is reduced again gradually upon further heating. The order-disorder or melting transition has a clear first-order nature, as can be seen from the hysteresis in the resistivity measurements. The peak intensities in the diffraction experiment showed much weaker hysteresis effect and therefore the most detailed experiments (Figs. 3 and 4) were carried out only during a very slow heating. The transition region between 260 and 280 K coincides with that observed in the resistivity during heating and it is likely that it corresponds to a region of coexistence between a fluidlike disordered phase and a solid phase. The same type hysteresis is seen in the variation of resistivity with pressure at ambient temperature where the transitions occur at 6 kbar.[13] Coexistence of this type has been observed at the melting transition for Kr and Xe adsorbed on graphite at coverages less than the commensurate value,[14,15] and it is also found in the phase diagrams that follow from computer simulation studies of lattice-gas models.[16] This leads us to a discussion of the relation between the theoretical lattice-gas models and their experimental counterparts. Both the adsorbed surface layer systems and the GIC have been analyzed by means of this analogy, and in both cases important shortcomings have been pointed out. The adsorbed systems are in general only weakly perturbed by the underlying lattice and there is not a very strong preference for particular adsorption sites. The alkaline metal GIC's have the metal atoms well localized at the centers of the carbon hexagons, but often the metal-metal interaction is so strong that the modulations appear in the graphite lattice, and in particular, it has been shown that the lattice-gas picture does not apply in the disordered state. The present system falls between these limits with a strong preference for particular site and sufficiently weak intercalant interactions so that the graphite lattice remains essentially unaltered through the different transitions. Furthermore, we have shown that the low-temperature structure has a clear 2D character, which suggests that this system may be a very good candidate for experimental exploration of the 2D four-state Potts model for which the equilibrium ordered state at a reduced density of 0.25 is the $(2\times2)R0°$ structure. C_9OsF_6 corresponds to a reduced density of 0.22 which, interestingly, is on the border of the stability of the (2×2) phase according to the renormalization-group analysis of this model with repulsive interactions.[11] Different staging and different choice of MF_6 molecules may allow further systematic study of the possible phases and phase diagrams of this model.

Our final comments concern the relation between the in-plane structure and the low-temperature residual resistivity which is found to vary with orders of magnitude both as a function of the staging and of the chemical composition.[9] Stage-1 C_9OsF_6 has a very high residual resistivity, and recent theoretical work by Ulloa and Kirczenow[17] has shown that it could be caused by incoherent electron scattering at defects of domain-wall character with separation on the scale of 10–100 Å. This is consistent with the picture that results from our structure analysis with the assumption that the disorder also affects the conduction in the graphite layers. It warrants further experimental as well as theoretical pursuit of this new and possibly very important mechanism for resistivity in this class of compounds.

VI. CONCLUSIONS

We have shown by neutron diffraction that the intercalant lattice in stage-1 C_9OsF_6 undergoes a transition from a completely disordered state above 300 K to an incommensurate, partly ordered 2D structure characterized by sharp domain walls arranged in a possibly weakly strained hexagonal lattice with a spacing of 60 Å. The low-temperature coherence length corresponds to a few of these lattice units. This structure corroborates a recent model of domain-wall scattering for the unusually high residual resistivity that is found in this compound. The order-disorder transition around 270 K has also been monitored by *c*-axis resistivity measurement as a function of both temperature and pressure and show clear hysteresis, indicative of a first-order transition. The low-temperature structure suggests that the OsF_6 molecules have strongly preferred sites and relatively weak repulsive interactions, which makes this class of compound a promising candidate for experimental realization of the lattice-gas version of the four-state Potts model in both 2D and 3D.

ACKNOWLEDGMENTS

Part of this work was carried out during mutual visits at Bar-Ilan University (J.K.) and at Risø National Laboratory (Y.Y.). Support from the respective institutions and from the Danish Natural Science Research Council is acknowledged. Partial support from the U.S.-Israel Binational Foundation under Grant No. 84-00192 is acknowledged.

[1]For a review on GIC see M. S. Dresselhaus and G. Dresselhaus, Adv. Phys. **30**, 175 (1981).
[2]P. Bak, Rep. Prog. Phys. **45**, 587 (1982).
[3]J. B. Hastings, J. P. Pouget, G. Shirane, A. J. Heeger, and A. G. MacDiarmid, Phys. Rev. Lett. **39**, 1484 (1977).
[4]P. A. Heiney, R. J. Birgeneau, G. S. Brown, P. M. Horn, D. E. Moncton, and P. W. Stephens, Phys. Rev. Lett. **48**, 104 (1982); S. G. J. Mochrie, A. R. Kortan, R. J. Birgeneau, and P. M. Horn, *ibid.* **53**, 985 (1984).
[5]H. Zabel, S. C. Moss, N. Caswell, and S. A. Solin, Phys. Rev. Lett. **43**, 2023 (1979); J. B. Hastings, W. D. Ellenson, J. E. Fischer, *ibid.* **42**, 1552 (1979); D. G. Onn, G. M. T. Foley, and J. E. Fischer, Phys. Rev. B **19**, 6474 (1979).
[6]S. A. Solin, Adv. Chem. Phys. **49**, 455 (1982).
[7]D. S. Robinson and M. B. Salamon, Phys. Rev. Lett. **48**, 156 (1982).
[8]N. Bartlett, E. M. McCarron, E. W. McQuillan, and P. E. Thompson, Synth. Met. **1**, 211 (1979).
[9]D. Vaknin, D. Davidov, H. Selig, V. Zevin, I. Felner, and Y. Yeshurun, Phys. Rev. B **31**, 3212 (1985).
[10]D. Vaknin, D. Davidov, H. Selig, and Y. Yeshurun, J. Chem. Phys. **83**, 3859 (1985); H. Selig, D. Vaknin, D. Davidov, and Y. Yeshurun, Synth. Met. **12**, 479 (1985); H. Selig, D. Vaknin, D. Davidov, and Y. Yeshurun, J. Chem. Soc. Chem. Commun. 1689 (1985).
[11]F. Y. Wu, Rev. Mod. Phys. **54**, 235 (1982).
[12]F. C. Frank and J. H. van der Merwe, Proc. R. Soc. London, Ser. A **198**, 216 (1949); Y. I. Frenkel and T. Kontorowa, Zh. Eksp. Teor. Fiz. **8**, 1340 (1938).
[13]D. Vaknin, D. Davidov, H. Selig, and D. Moses, in Proceedings of the Carbon Conference, Baden-Baden, 1986, edited by H. P. Boehm (unpublished).
[14]R. J. Birgeneau, E. M. Hammons, P. Heiney, P. W. Stephens, and P. M. Horn, in *Ordering in Two Dimensions* edited by S. K. Sinha (North-Holland, New York, 1980), and references therein.
[15]S. E. Nagler, P. M. Horn, T. F. Rosenbaum, R. J. Birgeneau, M. Sutton, S. G. Mochrie, D. E. Moncton, and R. Clarke, Phys. Rev. B **32**, 7373 (1985).
[16]A. N. Berker in *Ordering in Two Dimensions* edited by S. K. Sinha (North-Holland, New York, 1980); Y. Saito, Phys. Rev. B **26**, 6239 (1982).
[17]S. E. Ulloa and G. Kirczenow, Phys. Rev. Lett. **56**, 2537 (1986).